Impact of Remote Radio Head Positions on the Performance of Distributed Massive MIMO System with User Mobility

Habibullah Soomro and Aamir Habib
Dept. of Electrical Engineering, Institute of Space Technology, Islamabad, Pakistan
Emails: {habban_084@yahoo.com, aamir.habib@ist.edu.pk}

***Abstract*—The combination of interference mitigation, small cells and massive multiple-input multiple-output (MIMO) is the ultimate vision of future wireless technology. The combination of these three make a distributed massive MIMO system, in which the Base Station (BS) antennas are spread out over a large area, offering high coverage probability and less inter-cellular interference for cell-edge users as compared to a collocated massive MIMO system. The optimal configuration for remote radio heads (RRHs) in distributed massive MIMO is a challenge, which needs to be addressed. In this paper, we consider two scenarios for RRHs placement in a multi-cell distributed massive MIMO system. In the first case, RRHs are evenly placed on a circle of optimum radius. In the second case, RRHs are spatially distributed according to Poisson Point Process (PPP). The effect of both these layouts on different performance metrics including coverage, mobility, cost of deployment and interference is analyzed. Our work shows that placement of optimal circularly distributed RRHs outperform PPP distribution of RRHs in a multi-cell setting.**

***Index Terms*—distributed massive MIMO, user mobility, remote radio head, Poisson Point Process, circular distribution.**

I. Introduction

There is absolutely no denial to these two timeless facts: first, demand for wireless data rate will always rise; second, the amount of the existing electromagnetic spectrum will never grow. Therefore, techniques are required to use the available bandwidth more efficiently. Massive MIMO is one of these techniques [1]. Thomas Marzetta laid the foundation for this breakthrough technology in his ground-breaking research paper [2] published in November 2010.

In massive MIMO, the effects of frequency dependence and small-scale (*fast*) fading vanish due to channel hardening. This system requires inexpensive, low-power components and it provides robustness against deliberate jamming. It has the potential to increase the spectral efficiency ten times or more [3]. But *pilot contamination* in a multi-cellular environment is a major bottleneck in massive MIMO systems. Also, massive MIMO relies on *favorable propagation conditions* where the vector-valued channels from the base station to the single-antenna users are asymptotically orthogonal. Users at the edge of a cell experience low SNR due to the large distance between BS antenna array and cell-edge users [4]. Thus, the combination of interference mitigation, small cells and massive multiple-input multiple-output (MIMO) is the ultimate vision of future wireless technology. The combination of these three make a distributed massive MIMO system, in which the Base Station (BS) antennas are spread out over a large area [5], offering high coverage probability and less inter-cellular interference for cell-edge users as compared to a collocated massive MIMO system.

In a distributed massive MIMO system; the optimal configuration for remote radio heads (RRHs) is a challenge, which needs to be addressed. Reference [6] considers uplink massive MIMO system with distributed RRHs in a grid layout. A comparison is done between centralized massive MIMO and distributed massive MIMO systems in [6]. The attainable rate of a random immobile user terminal was derived in [7] for the case of circularly distributed massive MIMO system.

In this paper, we consider two scenarios for RRHs placement in a multi-cell distributed massive MIMO system with user mobility. In the first case, RRHs are evenly placed on a circle of optimum radius. In the second case, RRHs are spatially distributed according to Poisson Point Process (PPP). In [7], the distributed BS antennas are also evenly placed on a circle of optimum radius. But they have considered fixed users while we have analyzed user terminals with mobility. Also, they have considered circular cell while we have considered hexagonal cells.

The remainder of this paper is organized as follows. Section II introduces the system model and the effect of user mobility on channel characteristics. Section III describes the data transmission from the users to the RRHs and BS in each cell. Section IV describes the data transmission from the RRHs and BS to users in each cell. In Section V, simulation results are presented to compare the performance of circularly distributed RRHs with PPP distribution of RRHs. Finally, the conclusion for the optimal layout of RRHs placement is drawn in Section VI.

This paper uses the following notation: w is a scalar, $\mathbf{w}$ is a column vector, and $\mathbf{W}$ is a matrix. For a matrix, $\mathbf{W}^T$ is the transpose, $\mathbf{W}^*$ is the conjugate transpose, $\mathbf{W}^{-1}$ is the inverse, and $\mathbf{W}^H$ is the hermitian operation. The symbol $\|\mathbf{.}\|$ stands for the Euclidean norm. Finally, we use $z \sim \mathcal{CN}(0, \sigma^2)$ to denote a circularly symmetric complex Gaussian random variable (RV) z with zero mean and variance σ^2.

978-1-5386-3564-3/18/$31.00 ©2018 IEEE

II. System Model

A. Effect of User Mobility on Channel State Information

We consider the scenario of a multi-cellular[1] distributed massive MIMO system. In this model, the Base Station having M antennas is positioned at the center of each cell while the F RRHs are circularly or Poisson distributed. There are equal number of antennas N on each RRH and $M > N$. Therefore, the total number of antennas in each cell are,

$$J_l = M + NF \tag{1}$$

It is assumed that the RRHs are connected to the Base Station by high-capacity backhaul links such as fiber-optic cables. We employ time-division duplexing (TDD) on the uplink. In TDD, the downlink channels are obtained from the uplink channels through reciprocity [8]. There are different number of moving BS and RRH users in each hexagonal cell. Random Waypoint (RWP) mobility model has been chosen to incorporate the effects of mobility in the user terminals. In RWP, the user moves according to the following process [9]: -

$$\{(P_t^k, V_t^k, T_{p,t}^k)\}_{t\in N} = (P_1^k, V_1^k, T_{p,1}^k), (P_2^k, V_2^k, T_{p,2}^k), \dots \tag{2}$$

where P_t^k, V_t^k and $T_{p,t}^k$ denote the position, speed and pause time of user k at time instant t respectively. In RWP, a user moves from initial position (P_{t-1}) to next position (P_t) then pauses for $T_{p,t}$ before changing its direction. For a given area, a higher speed causes the mobile user to change its direction frequently. Let d_t^k indicate the location of user k at time t with respect to the BS given by,

$$d_t^k = \|P_t^k - P^{BS}\| \tag{3}$$

where P^{BS} is the position of BS, which is fixed.

B. Channel Model for Base Station User

Let $g_{lk}^m(t)$ denote the channel coefficient from the k^{th} BS user in the l^{th} cell to the m^{th} BS antenna at time instant t. We assume that,

$$g_{lk}^m(t) = \sqrt{\beta_{lk}(d_t^k)}\, h_{lk}^m(t) \qquad l = 1, \dots, L \tag{4}$$

where $h_{lk}^m \sim \mathcal{CN}(0,1)$ is small-scale (*fast*) fading and β_{lk} is large-scale (*slow*) fading at different user locations. As seen in (4), large-scale fading does not depend upon BS antenna index m. Perfect channel state information (CSI) is assumed at the BS. The $M \times K$ matrix of channel coefficients from all BS user terminals in the l^{th} cell to BS antennas of that cell at time t is given by:

$$\mathbf{G}_l(t) = \begin{bmatrix} g_{l1}^1(t) & \dots & g_{lK}^1(t) \\ \vdots & \ddots & \vdots \\ g_{l1}^M(t) & \dots & g_{lK}^M(t) \end{bmatrix} \tag{5}$$

[1]We have considered hexagonal cells in our analysis.

C. Channel Model for Remote Radio Head User

Let $q_{lu}^{fn}(t)$ denote the channel coefficient from the u^{th} RRH user in the l^{th} cell to the n^{th} antenna of RRH index f at time instant t. We will follow the same assumption for fading and CSI as in the case of Subsection II-B. The only modification is that large-scale fading coefficient β also depends upon RRH index f. Similar to Subsection II-B, the $NF \times U$ matrix of channel coefficients from all RRH user terminals in the l^{th} cell to antennas of all the RRHs at time t is given by $\mathbf{Q}_l(t)$.

III. Reverse-Link Data Transmission

A. Reverse-link for Base Station Users

The signal received at the m^{th} base station antenna in the l^{th} cell at time t is a superposition of signals transmitted from the K BS user terminals in the l^{th} cell and the interfering U RRH user terminals of that same cell. For exposition ease, interference from users in other cells is overlooked. Mathematically,

$$y_{lm}(t) = \sum_{k=1}^{K} g_{lk}^m(t) x_{lk}(t) + \underbrace{\sum_{f=1}^{F}\sum_{u=1}^{U} q_{lu}^{fn}(t) s_{lu}(t)}_{\text{RRH users interference}} + w_{lm}(t) \tag{6}$$

where $x_{lk}(t)$ and $s_{lu}(t)$ is the data transmitted by the k^{th} BS user and the u^{th} RRH user at time instant t in the l^{th} cell repectively. The last term in (6), $w_{lm}(t)$, represents additive receiver noise, which we assume is $\sim \mathcal{CN}(0,1)$. In vector form,

$$\mathbf{y}_l(t) = \mathbf{G}_l(t)\, \boldsymbol{x}_l(t) + \mathbf{Q}_l(t)\, \mathbf{s}_l(t) + \mathbf{w}_l(t) \tag{7}$$

where $\mathbf{y}_l(t) = [y_{l1}(t), \dots, y_{lM}(t)]^T$, $\mathbf{w}_l(t) = [w_{l1}(t), \dots, w_{lM}(t)]^T$, $\boldsymbol{x}_l(t) = [x_{l1}(t), \dots, x_{lK}(t)]^T$ and $\mathbf{s}_l(t) = [s_{l1}(t), \dots, s_{lU}(t)]^T$.

Zero-forcing (ZF): In massive MIMO, the required signal processing simplifies. Hence, low-complexity detectors also give optimum performance. Here, we use ZF to separate data streams from different BS users in each cell. ZF uses the following $M \times K$ pseudoinverse $\mathbf{A}$ as the decoding matrix:

$$\mathbf{A}_l = \mathbf{G}_l(t)\, \left\{\mathbf{G}_l^H(t)\mathbf{G}_l(t)\right\}^{-1} \tag{8}$$

The received signal (7) is processed by multiplying it by (8),

$$\begin{aligned} \mathbf{A}_l^H \mathbf{y}_l(t) = {} & \left\{\mathbf{G}_l^H(t)\mathbf{G}_l(t)\right\}^{-1} \mathbf{G}_l^H(t)\, \mathbf{G}_l(t)\, \boldsymbol{x}_l(t) \\ & + \left\{\mathbf{G}_l^H(t)\mathbf{G}_l(t)\right\}^{-1} \mathbf{G}_l^H(t)\, \mathbf{Q}_l(t)\, \mathbf{s}_l(t) \\ & + \left\{\mathbf{G}_l^H(t)\mathbf{G}_l(t)\right\}^{-1} \mathbf{G}_l^H(t)\, \mathbf{w}_l(t) \end{aligned} \tag{9}$$

$$\begin{aligned} \left[\mathbf{A}_l^H \mathbf{y}_l(t)\right]_k = {} & x_{lk}(t) + \left[\left\{\mathbf{G}_l^H(t)\mathbf{G}_l(t)\right\}^{-1} \mathbf{G}_l^H(t)\mathbf{Q}_l(t)\mathbf{s}_l(t)\right]_k \\ & + \left[\left\{\mathbf{G}_l^H(t)\mathbf{G}_l(t)\right\}^{-1} \mathbf{G}_l^H(t)\, \mathbf{w}_l(t)\right]_k \end{aligned} \tag{10}$$

TABLE I
SIMULATION PARAMETERS FOR CIRCULARLY DISTRIBUTED REMOTE RADIO HEADS

Parameter	Value	Parameter	Value
Cell radius	235 m	Simulation time	600 secs
Pathloss exponent	4	Simulation area	1 km^2
RRH coverage	50 m	User speed	0.5 to 1.6 m/s
Optimum radius of circle	179.36 m	Walk time	10 to 25 secs
RRHs in each cell	5	Pause time	0 to 30 secs

B. Reverse-link for Remote Radio Head Users

The signal received at the n^{th} antenna of RRH f in the l^{th} cell at time instant t is given by,

$$r_{ln,f}(t) = q_{lu}^{fn}(t)s_{lu}(t) + \underbrace{\sum_{\substack{f'=1\\f'\neq f}}^{F}\sum_{\substack{u'=1\\u'\neq u}}^{U} q_{lu'}^{f'n}(t)s_{lu'}(t)}_{\text{interference from other RRH users}} + \underbrace{\sum_{k=1}^{K} g_{lk}^{m}(t)x_{lk}(t)}_{\text{BS users interference}} + b_{ln,f}(t) \quad (11)$$

In vector form,

$$\mathbf{r}_{l,f}(t) = \mathbf{q}_{lu}^{f}(t)\, s_{lu}(t) + \mathbf{Q}_{l}^{f\prime}(t)\, \mathbf{s}_{l}^{u\prime}(t) + \mathbf{G}_{l}(t)\, \boldsymbol{x}_{l}(t) + \mathbf{b}_{l,f}(t) \quad (12)$$

where $\mathbf{r}_{l,f}(t) = [r_{l1,f}(t), \ldots, r_{lN,f}(t)]^T$ and $\mathbf{q}_{lu}^{f}(t) = [q_{lu}^{f1}(t), \ldots, q_{lu}^{fN}(t)]^T$.

IV. Forward-Link Data Transmission

A. Forward-link for Base Station Users

Same as before in Subsection III-A, interference from adjoining base stations is overlooked. Under the assumption of reciprocity, the k^{th} BS user in the l^{th} cell at time t receives,

$$y_{lk}(t) = \sum_{m=1}^{M} g_{lk}^{mT}(t)\tilde{x}_{lm}(t) + \underbrace{\sum_{f=1}^{F}\sum_{n=1}^{N} q_{lu}^{fnT}(t)s_{ln,f}(t)}_{\text{RRH antennas interference}} + w_{lk}(t) \quad (13)$$

where $\tilde{x}_{lm}(t)$ and $s_{ln,f}(t)$ represents the data transmitted by the m^{th} BS antenna and the n^{th} antenna of RRH index f at time instant t in the l^{th} cell repectively. $w_{lk}(t)$ is noise with distribution $\sim \mathcal{CN}(0,1)$. Collectively, the K BS user terminals in the l^{th} cell at time t will receive the $K \times 1$ vector,

$$\begin{aligned}\mathbf{y}_{l}(t) &= \mathbf{G}_{l}^{T}(t)\, \tilde{\boldsymbol{x}}_{l}(t) + \mathbf{Q}_{l}^{T}(t)\, \mathbf{s}_{l}(t) + \mathbf{w}_{l}(t) \\ &= \mathbf{G}_{l}^{T}(t)\, \mathbf{A}_{l}\, \boldsymbol{x}_{l}(t) + \mathbf{Q}_{l}^{T}(t)\, \mathbf{s}_{l}(t) + \mathbf{w}_{l}(t) \end{aligned} \quad (14)$$

where $\mathbf{y}_l(t) = [y_{l1}(t), \ldots, y_{lK}(t)]^T$, $\mathbf{w}_l(t) = [w_{l1}(t), \ldots, w_{lK}(t)]^T$, $\boldsymbol{x}_l(t) = [x_{l1}(t), \ldots, x_{lM}(t)]^T$ and $\mathbf{s}_l(t) = [s_{l1,1}(t), \ldots, s_{lN,F}(t)]^T$.

Zero-forcing (ZF): ZF uses the following precoding matrix,

$$\mathbf{A}_l = \sqrt{M-K}\, \mathbf{G}_{l}^{*}(t) \left\{\mathbf{G}_{l}^{T}(t)\mathbf{G}_{l}^{*}(t)\right\}^{-1} \quad (15)$$

The substitution of precoding matrix (15) into (14) yields,

$$\mathbf{y}_{l}(t) = \sqrt{M-K}\, \boldsymbol{x}_{l}(t) + \mathbf{Q}_{l}^{T}(t)\, \mathbf{s}_{l}(t) + \mathbf{w}_{l}(t) \quad (16)$$

B. Forward-link for Remote Radio Head Users

Under the assumption of reciprocity, the u^{th} RRH user in the l^{th} cell at time t receives,

$$r_{lu}(t) = \sum_{n=1}^{N} q_{lu}^{fnT}(t)s_{ln,f}(t) + \underbrace{\sum_{\substack{f'=1\\f'\neq f}}^{F}\sum_{n=1}^{N} q_{lu}^{f'nT}(t)s_{ln,f'}(t)}_{\text{interference from other RRH antennas}} + \underbrace{\sum_{m=1}^{M} g_{lk}^{mT}(t)\tilde{x}_{lm}(t)}_{\text{BS antennas interference}} + b_{lu}(t) \quad (17)$$

Collectively, the U RRH user terminals in the l^{th} cell at time t will receive,

$$\mathbf{r}_{l}(t) = \mathbf{q}_{lu}^{fT}(t)\, \mathbf{s}_{l,f}(t) + \mathbf{Q}_{l}^{f'T}(t)\, \mathbf{s}_{l,f'}(t) + \mathbf{G}_{l}^{T}(t)\, \tilde{\boldsymbol{x}}_{l}(t) + \mathbf{b}_{l}(t) \quad (18)$$

V. Numerical Evaluations

In this section, we present simulation results to compare the performance of circularly distributed RRHs with PPP distribution of RRHs in distributed massive MIMO system. The Base station having M antennas is placed at the center of each hexagonal cell for both the layouts. The coverage range of the RRHs, mobility characteristics of the user terminals, simulation time and simulation area are also the same. We have considered the mobility of pedestrians whose average speed is 5 km/h.

A. Circularly Distributed Remote Radio Heads

In each cell, 5 RRHs are evenly placed on a circle of optimum radius. See the Appendix for details on the optimum radius. There are equal number of antennas N on each RRH and BS antennas are greater than RRHs antennas. For the initial random placement of users, a minimum distance of 50 metres has been maintained between a BS antenna and a user in each cell. But there is no such restriction after the simulation for the mobility of users has started. The results

TABLE II
SIMULATION PARAMETERS FOR POISSON POINT PROCESS DISTRIBUTION OF REMOTE RADIO HEADS

Parameter	Value	Parameter	Value
Area of cell	1.43×10^5 m^2	Simulation time	600 secs
Pathloss exponent	4	Simulation area	1 km^2
RRH coverage	50 m	User speed	0.5 to 1.6 m/s
Min distance b/w RRH and BS	70 m	Walk time	10 to 25 secs
RRH density	4.89×10^{-5} RRHs/m^2	Pause time	0 to 30 secs

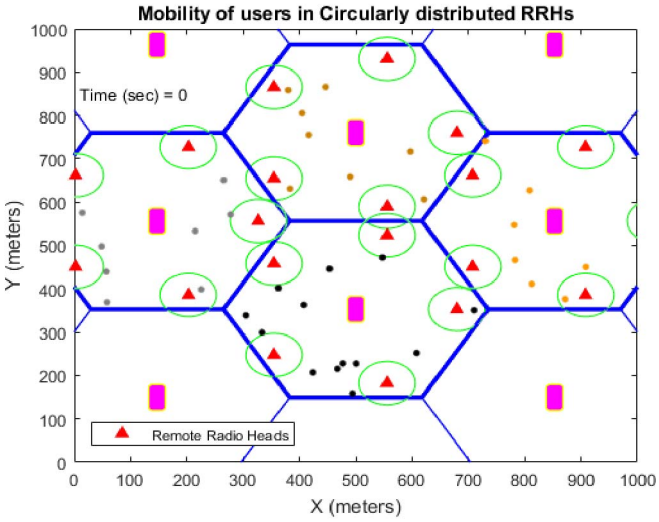

(a) $t = 0$ secs

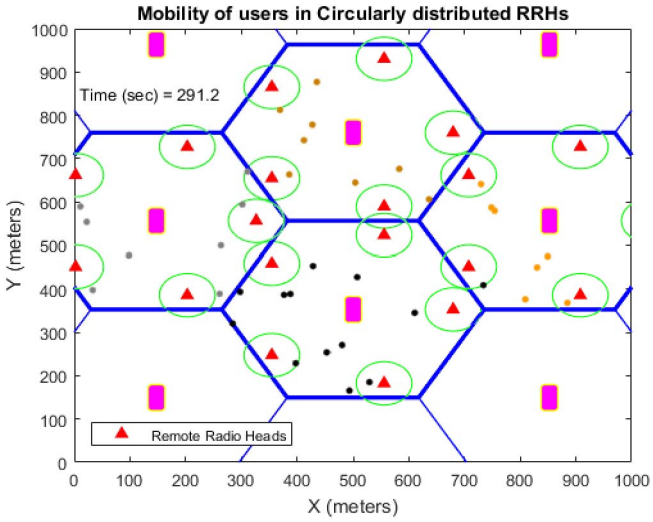

(b) $t = 300$ secs

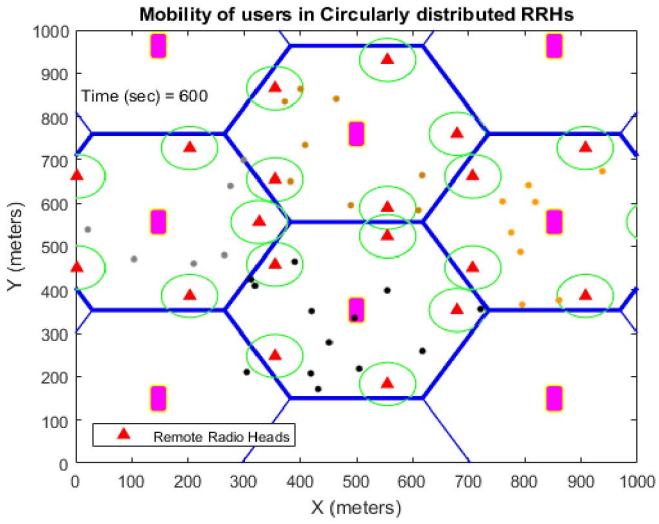

(c) $t = 600$ secs

Fig. 1. Position of moving user terminals at different time instances during the continuous simulation.

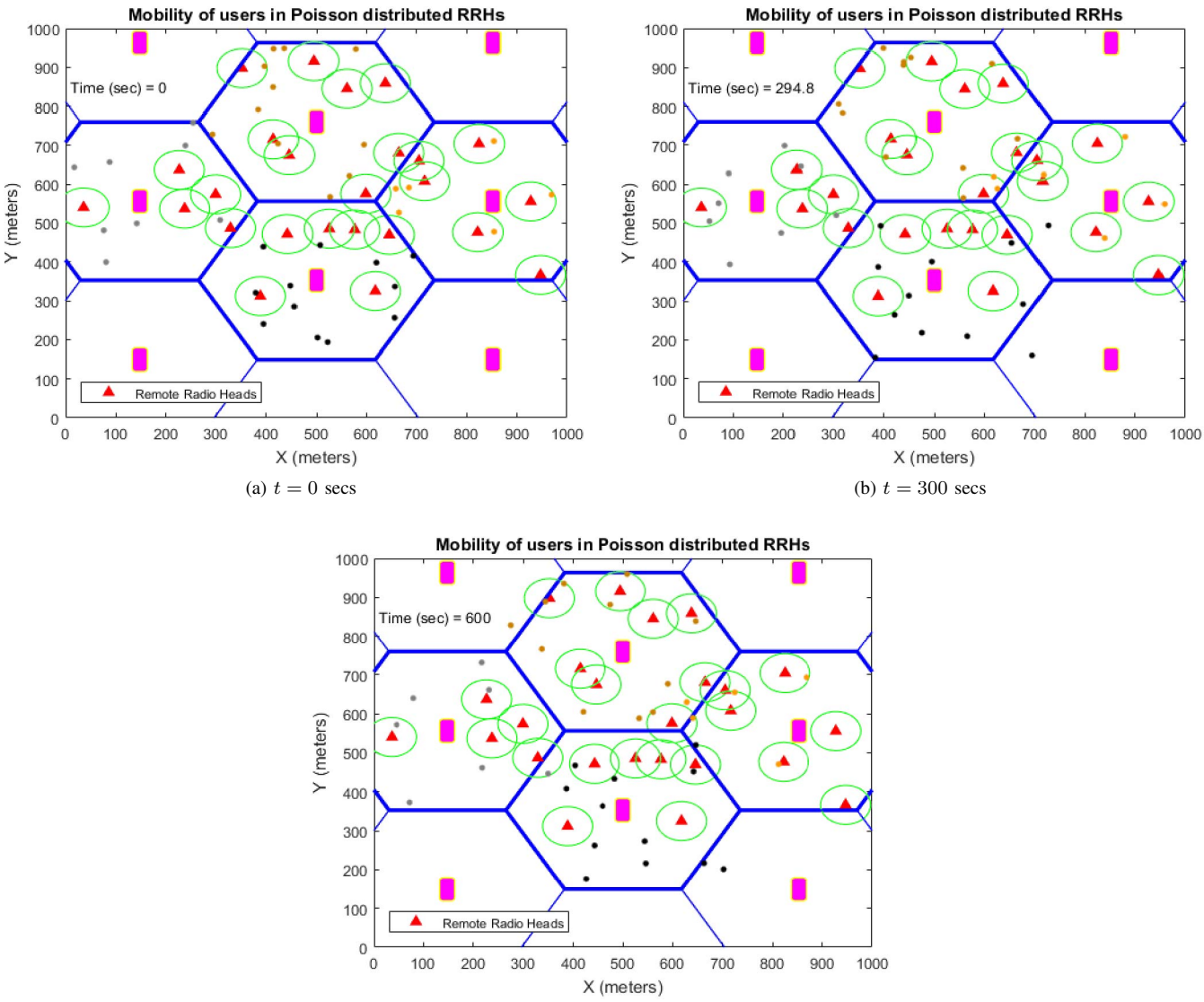

(a) $t = 0$ secs

(b) $t = 300$ secs

(c) $t = 600$ secs

Fig. 2. Position of moving user terminals at different time instances during the continuous simulation.

are obtained for the parameter setting summarized in Table I. The simulations were performed using MATLAB software.

Fig. 1 shows some snapshots from the continuous 10 minutes simulation of moving users. Fig. 1(a) depicts the initial position of users. Fig. 1(b) shows their position after 5 minutes. Finally, Fig. 1(c) shows the position of users after the simulation time has completed. The users of each cell have been given a distinct color for better visualization. As it can be seen in Fig. 1, many of the cell-edge users at any time instant are within the coverage area of RRHs. While those users around the center of the cell will receive good coverage from the BS. There is hardly any overlapping between the coverage area of RRHs. Hence, a RRH user will have negligible interference from other RRH antennas. The coverage for the cell-edge users can be further improved by installing more RRHs but this will increase the cost of infrastructure.

B. Poisson Point Process Distribution of Remote Radio Heads

In this model, the RRHs are distributed in each cell according to PPP of density $\lambda = 4.89 \times 10^{-5}$ (measured in RRHs per m^2). The number of RRHs in any area of size A is a Poisson distributed stochastic variable with mean value λA [10]. In our case, the mean value for the number of RRHs in a cell is 7. We will follow the same settings for RRH antennas and initial position of users as in Subsection V-A. The results are obtained for the parameter setting summarized in Table II.

Fig. 2 shows some snapshots from the continuous 10 minutes simulation of moving users. Fig. 2 (a) depicts the initial position of users. Fig. 2 (b) shows their position after 5 minutes. Finally, Fig. 2 (c) shows the position of users after the simulation time has completed. There are more RRHs in

each cell than in Subsection V-A. But still most of the users are out of the coverage area of RRHs at any time t in Fig. 2. This will increase the load on BS antenna array. A minimum distance of 70 metres has been maintained between a RRH and the BS as shown by Fig. 2. This has been done to avoid severe interference from BS antenna array towards RRH users. There is too much overlapping between the coverage areas of RRHs. Hence, a RRH user will have great interference from other RRH antennas. This affects the data rate of RRH users and defeats the purpose of using distributed massive MIMO system.

VI. Conclusion

In this paper, we have considered multi-cellular distributed massive MIMO system with user mobility. The ZF detection and precoding is used at the BS. We have considered two scenarios for the placement of remote radio heads in each cell; circular and PPP distribution. The performance of the system with respect to different parameters such as infrastructure cost, coverage and interference has been compared for both the cases. Our work has shown that placement of optimal circularly distributed RRHs outperform PPP distribution of RRHs. Our obtained results can assist infrastructure providers in the optimal placement of RRHs in distributed massive MIMO systems in practice.

Appendix
Optimum Radius

The radius of the circular BS antenna array for the distributed massive MIMO system that maximizes asymptotic average achievable rate per user is [7]:

$$r_{opt} = \sqrt{\frac{R^2}{t_0 + 1}} \tag{A.19}$$

where R is cell radius and t_0 is the solution of the following equation:

$$x^{3+\frac{2}{v-2}} + 2x^{2+\frac{2}{v-2}} - 1 = 0 \tag{A.20}$$

The equation in (A.20) only depends on the path-loss exponent v and can be easily solved offline by software such as MATLAB.

References

[1] T. L. Marzetta, E. G. Larsson, H. Yang, and H. Q. Ngo, *Fundamentals of Massive MIMO*. Cambridge, UK: Cambridge University Press, 2016.

[2] T. L. Marzetta, "Noncooperative cellular wireless with unlimited numbers of base station antennas," *IEEE Trans. Wireless Commun.*, vol. 9, pp. 3590–3600, Nov. 2010.

[3] E. G. Larsson, O. Edfors, F. Tufvesson, and T. L. Marzetta, "Massive mimo for next generation wireless systems," *IEEE Commun. Mag.*, vol. 52, pp. 186–195, Feb. 2014.

[4] F. Rusek, D. Persson, B. K. Lau, E. G. Larsson, T. L. Marzetta, O. Edfors, and F. Tufvesson, "Scaling up mimo: Opportunities and challenges with very large arrays," *IEEE Signal Process. Mag.*, vol. 30, pp. 40–60, Jan. 2013.

[5] K. T. Truong and R. W. Heath, "The viability of distributed antennas for massive mimo systems," in *Signals, Systems and Computers, 2013 Asilomar Conference on*, pp. 1318–1323, IEEE, 2013.

[6] E. Björnson, M. Matthaiou, and M. Debbah, "Massive mimo with non-ideal arbitrary arrays: Hardware scaling laws and circuit-aware design," *IEEE Trans. Wireless Commun.*, vol. 14, pp. 4353–4368, Apr. 2015.

[7] A. Yang, Y. Jing, C. Xing, Z. Fei, and J. Kuang, "Performance analysis and location optimization for massive mimo systems with circularly distributed antennas," *IEEE Trans. Wireless Commun.*, vol. 14, pp. 5659–5671, Oct. 2015.

[8] T. L. Marzetta, "Massive mimo: an introduction," *Bell Labs Tech. J.*, vol. 20, pp. 11–22, Mar. 2015.

[9] R. R. Roy, *Handbook of mobile ad hoc networks for mobility models*. Springer Science & Business Media, 2010.

[10] E. Björnson, L. Sanguinetti, and M. Kountouris, "Deploying dense networks for maximal energy efficiency: Small cells meet massive mimo," *IEEE J. Sel. Areas Commun.*, vol. 34, pp. 832–847, Apr. 2016.